

presented at the Applications of Lasers to Industrial Chemistry Symposium at the
1984 SPIE meeting in January, Los Angeles, CA
appear in the proceedings for the "Applications of Lasers to Industrial
Chemistry Symposium, January 1984"

a-Si:H films produced from laser heated gases:
process characteristics and film properties

J. H. Flint, M. Meunier, J. Adler and J. S. Haggerty

77 Massachusetts Avenue, 12-009
Massachusetts Institute of Technology, Cambridge, MA 02139

Abstract

A process for depositing a-Si:H films from CO₂ laser-heated gases has been demonstrated and modelled; the properties of resulting films have been investigated extensively. Film growth rate is determined by the peak gas temperature, defined by an energy balance between the absorption of the laser beam and thermal conduction to the substrate and the cell walls. The hydrogen content and neutral spin density follow an equilibrium function of the substrate temperature. The optical and electronic properties also depend on the substrate temperature.

Introduction

There has been increasing interest recently in thin films produced by laser irradiation of gases.¹ For most film deposition processes, the laser beam intersects the substrate. This may cause the reaction kinetics to be dominated by heterogeneous processes,² and it introduces an ambiguity with respect to the partition of the absorbed laser energy between the reactant gas and the substrate.³ The process described in this paper directs a laser beam through an absorbing gas parallel to the substrate upon which the film is deposited, Figure 1.^{4,5} The reactant gas temperature is controlled independent of the substrate temperature. This decouples the film properties from the film growth rate. Bilenchi et al.⁶ have also produced a-Si:H and West et al.⁷ have produced silicon nitride using this technique.

We anticipated that the LICVD process would be thermally activated, with the film growth rate controlled by the thermal dissociation of SiH₄; thus, it should be exponentially dependent on the peak gas temperature (T_g). In contrast, the film properties should primarily be a function of the substrate temperature (T_s). In this paper, we present experimental data and theoretical analysis which verifies these presumptions and quantifies the relationships between process variables and both process and film characteristics.

Process characterization

The characteristics of the LICVD process have been modelled empirically and analytically.⁸ Empirical characterization involved systematic manipulation of process variables and the observation of their effects on growth rate and other process and film characteristics. The variables studied include gas composition, gas pressure, gas flow rate, laser power, laser intensity, beam-substrate spacing and substrate temperature. It is evident that the growth rate is directly related to the peak gas temperature now that relationships between peak gas temperature and process variables have been developed. Our process modelling consists of verifying the thermalization of the absorbed laser energy, calculating peak gas temperatures, stating probable molecular reactions, and measuring growth rates in terms of appropriate process variables.

Thermalization of absorbed photon energy

When an infrared photon is absorbed, the SiH₄ molecule makes a transition to an excited vibrational level. Collisions redistribute the absorbed energy returning the absorbing molecule to its ground state where it is again able to absorb another photon. For LICVD conditions (~ 1 watt absorbed/cm, $P_{SiH_4} \sim 10$ torr and $T_g \sim 800K$), a molecule

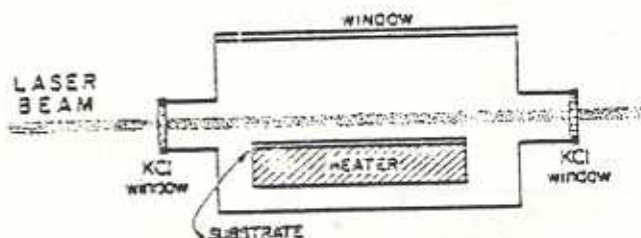


Fig. 1. Schematic of the LICVD reactor.

absorbs a photon every 700 μ s and the average time between collisions is 0.015 μ s. Vibrational-vibrational (V-V), vibrational-rotational (V-R), and rotational-translational (R-T) relaxation times are 0.5 μ s, 100 μ s, and 0.1 μ s respectively.^{9,10} Therefore, most of the molecules experience sufficient collisions to relax to a state where the absorbed vibrational energy is distributed equally among the various degrees of freedom of the molecule. Thus, under the conditions employed in LICVD, the overall effect of absorbing IR photons is simply to increase the gas temperature.

Peak gas temperature

The peak gas temperature, T_g , can be calculated from a steady-state energy balance between the energy absorbed by the gas and the energy lost by thermal conduction. For a highly simplified system geometry, the steady-state energy balance equation is

$$W\alpha = \frac{2\pi}{\ln(2D/r)} \kappa (T_g - T_s) \quad (\text{watts/cm}) \quad (1)$$

where T_g is the gas temperature, T_s is the substrate temperature, κ is the thermal conductivity of the gas, α is the absorptivity of the gas, and W is the laser power. $2\pi/\ln(2D/r)$ is the thermal conduction shape factor for an isothermal cylinder (the laser beam) of radius r a distance D from an isothermal surface (the substrate).¹¹

The absorptivity, α , depends on the number of absorbing molecules ($P_{SiH_4} = P$), the frequency difference between the laser line and the SiH_4 absorption line, and the respective line widths.¹² With LICVD processing conditions, the principal source of line overlap results from pressure broadening, which is approximately proportional to the SiH_4 pressure, P . Therefore, α is proportional to the square of the SiH_4 pressure:

$$\alpha = \alpha_0 P^2 \quad (2)$$

Equation (1) can be rewritten in a form that illustrates how the gas temperature depends on the various experimental parameters:

$$T_g = T_s + \frac{\ln(2D/r)}{2\pi\kappa} W \alpha_0 P^2 \quad (3)$$

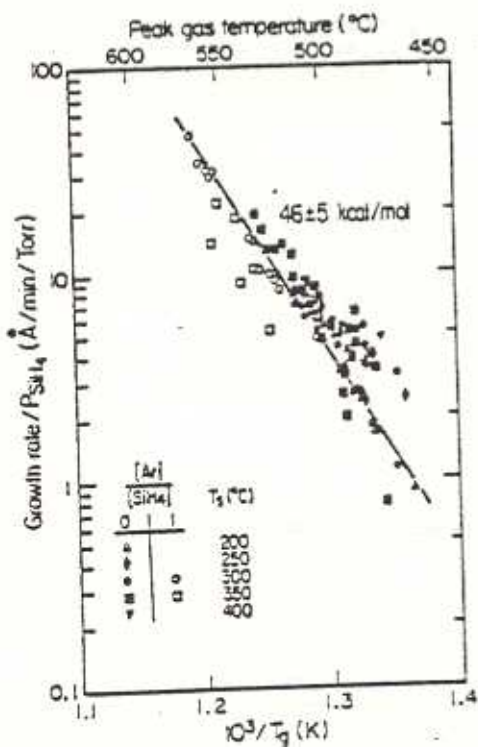


Fig. 2. Arrhenius plot of growth rate, $\text{\AA}/\text{min}$ per torr of SiH_4 , as a function of reciprocal calculated peak gas temperature for films made with various LICVD processing conditions.

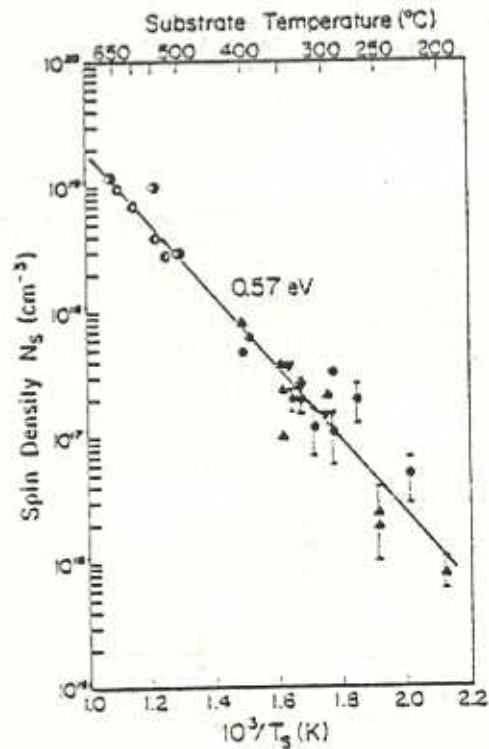


Fig. 3. Spin Density, N_3 , vs $1/T_s$ for LICVD films, \bullet 25W, \blacktriangle 40W, ∇ 45W local laser powers at positions above the substrate and for normal CVD films 3, 17, 0.¹³

Equation (3) indicates that T_g is dependent on the laser power (W), the square of the silane pressure, and inversely dependent on the gas thermal conductivity. To calculate T_g accurately we have solved a more general version of Equation (3), using temperature dependent values for α and κ , and our complete system geometry.³ For the range of conditions used to deposit films, calculated gas temperatures range from approximately 450°C to 575°C.

Reaction mechanism

Analogous to the HOMOCVD growth model proposed by Scott et al.,¹³ we propose a model for LICVD in which the rate-limiting step is homogeneous thermal decomposition of the SiH_4 :



If SiH_4 decomposition is the rate-limiting step, the film growth rate G can be expressed as:

$$G = P_{SiH_4} e^{-E/kT_g} \quad (5)$$

where E is the activation energy of the decomposition reaction. According to kinetic studies of homogeneous SiH_4 decomposition, the activation energy is 52-56 kcal/mole.¹⁴

Growth rate kinetics

Figure 2 summarizes the results of 80 a-Si:H film growth runs made under different process conditions; variables include laser power, gas pressure, gas composition, and substrate temperature. The growth rate per torr SiH_4 follows the Arrhenius dependence on T_g predicted by Equation (5).

The value of the observed activation energy, 46 ± 5 kcal/mole, is slightly lower than the 52-56 kcal/mole reported for the pyrolysis of SiH_4 . However, it is much higher than the ~ 35 kcal/mole reported for conventional CVD growth of Si from SiH_4 for which the rate-limiting step is reported to be surface diffusion.¹⁵ Acknowledging the potential errors in calculated LICVD peak gas temperatures, we believe that the observed activation energy is in sufficient agreement with the higher values to conclude the process is indeed rate-controlled by SiH_4 dissociation.

Film properties

Adherent films have been deposited on fused silica, borosilicate glass, aluminum, and single-crystal silicon. All films were determined to be amorphous by electron diffraction, as expected from the low substrate temperatures used ($T_s < 400^\circ C$). Films 1 μm thick at the center of 2.5 cm x 5.0 cm substrates are typically 0.3 μm thick at the edges.

The concentration of unpaired spins, N_s , which can be evaluated by electron spin resonance (ESR), provides an important measure of the quality of the a-Si:H films.¹⁶ If N_s is too large, the resulting defect states pin the Fermi level, precluding the fabrication of high-quality semiconductor devices. The incorporation of hydrogen in a-Si films ordinarily decreases the defect concentration sufficiently to allow variation of the Fermi level by substitutional doping. Figure 3 shows an Arrhenius plot of N_s versus the substrate temperature for a-Si:H films deposited by the LICVD process. Values for conventional CVD films are also included.^{17,18} The observed g value is ~ 2.0055, indicative of neutral dangling bonds.¹⁹ The lowest N_s obtained thus far is ~ $8 \times 10^{15} cm^{-3}$, which is nearly the same as the best films produced by glow-discharge¹⁹ and HOMOCVD techniques.²⁰ The fact that CVD and LICVD values are on the same line emphasizes the similarity of the two processes. Moreover, the Arrhenius plot is quite linear which indicates that the residual dangling-bond concentration is in thermal equilibrium at the substrate temperature, the activation energy being 0.57 eV (13.2 kcal/mole). The explanation for this phenomenon is not yet clear, but we presently believe it is a consequence of the growth mechanism.

The hydrogen concentration, [H], was determined by the effusion technique.¹⁹ Kampas and Griffith²¹ have proposed a model for the growth of a-Si:H films which relates the ratio of the rates of $-SiH_3$ deactivation, r_1 , and hydrogen elimination, r_2 , to the function $[H]^{-1-3}$. An Arrhenius plot of this function versus T_s is shown in Figure 4 for both LICVD films and conventional CVD films.²¹ The plot is reasonably linear with an activation energy of 0.59 eV. This value, essentially the same as for dangling bond creation, represents the difference in activation energies of the hydrogen elimination and $-SiH_3$ deactivation processes.

Figure 5 shows the optical gap, E_{opt} , as deduced from the Tauc expression²² as a function of T_s for LICVD and conventional CVD films.²⁴ The increase of E_{opt} with decreasing T_s is most likely due to the increasing [H] concentration in the films, since the Si-H bond strength (~ 3.4 eV) is greater than the Si-Si bond strength (~ 2.4 eV).²⁵

Although not explained mechanistically, these results indicate that the spin density, the hydrogen content and the optical gap are functions of T_s only. The primary dependence of these film characteristics on T_s was anticipated; the Arrhenius functional dependence for $[H]$ and N_s was not.

Preliminary conductivity and photoconductivity measurements have been completed on two films deposited across aluminum electrodes. The dark conductivities were very small ($\sim 10^{-11} (\Omega \text{ cm})^{-1}$), and were thermally activated. The conductivities increased by over 2×10^4 when the films were exposed to $\sim 100 \text{ mW/cm}^2$ of red light (600 nm to 1100 nm). The film deposited at 200°C demonstrated the Staebler-Wronski effect,¹⁹ but the one deposited at 350°C did not. These results suggest that the Fermi level lies near the center of the gap for our undoped films. Doping experiments are now being planned to produce films with high dark conductivities.

Discussion and conclusions

Most of the presumed attributes of the LICVD process have been demonstrated with a-Si:H films deposited from SiH_4 . The growth process is controlled by the thermally activated dissociation of SiH_4 at a rate determined by the peak gas temperature. The peak gas temperature is established by the balance between the energy absorbed by the gas molecules and that lost to surrounding surfaces by thermal conduction. The film properties are determined by the substrate temperature. It is through independent control of T_g and T_s that LICVD uniquely permits optimization of growth and film properties.

Acknowledgments

The financial support of the 3M Corp., SOHIO, the NRC of Canada and the MIT Materials Processing Center is gratefully acknowledged. We would also like to acknowledge the contributions of Eric Ting-Shan Pan.

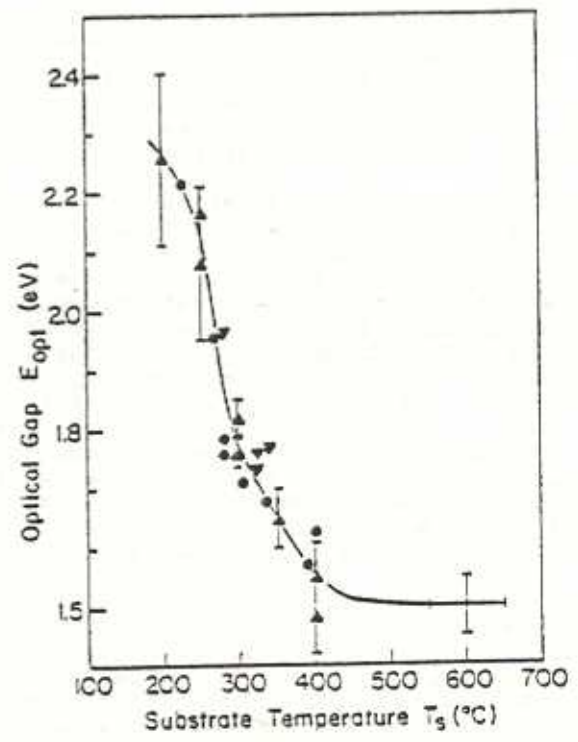
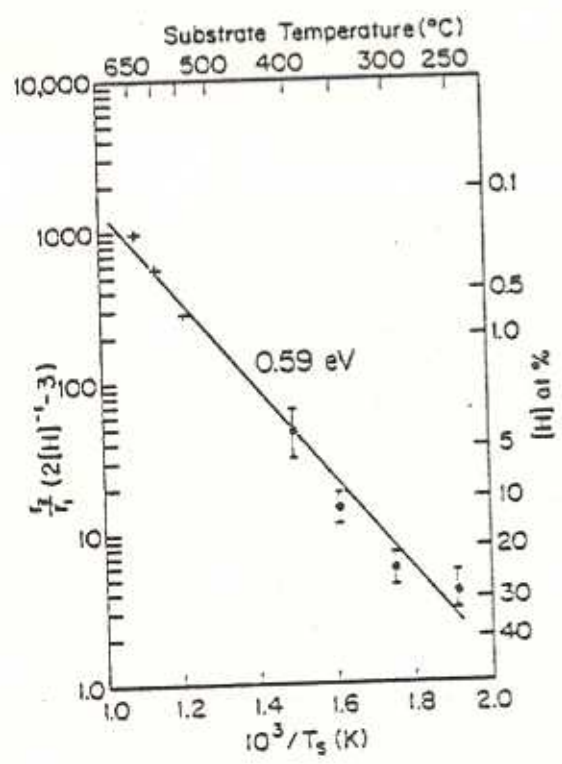


Fig. 4. $2[H]^{-1/3}$ vs $1/T_s$ for LICVD and conventional CVD²² films.

Fig. 5. E_{opt} as a function of T_s for the same LICVD films as in Fig. 3, and for conventional CVD films (+).²⁴

References

1. Materials Research Society Symposia Proceedings, Laser Diagnostics and Photochemical Processing for Semiconductor Devices, 17, R. M. Osgood, S. R. J. Brueck and H. R. Schlossberg, eds. (North Holland 1983).
2. C. P. Christensen and K. M. Lakin, Appl. Phys. Lett., 32, 254 (1978).
3. M. Hanabusa, A. Namiki, K. Yoshinara, Appl. Phys. Lett., 35, 626 (1979).
4. T. R. Gattuso, M. Meunier, D. Adler and J. S. Haggerty in Ref. 1, pp. 215-22.
5. M. Meunier, T. R. Gattuso, D. Adler and J. S. Haggerty, Appl. Phys. Lett., 43, 273-5 (1983).
6. R. Bilenchi, I. Gianinoni and M. Musci, J. Appl. Phys., 53, 6479-81 (1982).
7. G. A. West and A. Gupta, Materials Research Society Symposia Proceedings, Laser-Controlled Chemical Processing of Surfaces, A. W. Johnson and D. J. Ehrlich, eds., (in press).
8. M. Meunier, J. H. Flint, D. Adler, and J. S. Haggerty, Materials Research Society Symposia Proceedings, Laser-Controlled Chemical Processing of Surfaces, A. W. Johnson and D. J. Ehrlich, eds., (in press).
9. P. A. Longeway and F. W. Lampe, J. Am. Chem. Soc., 103, 6813-8 (1981).
10. R. D. Levine and R. B. Bernstein, Molecular Radiation Dynamics (Oxford University Press, NY, Chap. 5, 1974).
11. J. P. Holman, Heat Transfer, (McGraw-Hill, NY, NY 1976).
12. A. C. G. Mitchell and M. W. Zemansky, Resonance Radiation and Excited Atoms, (Cambridge University Press, Cambridge, U. K. 1961).
13. B. A. Scott, R. M. Plecenik and E. E. Simonyi, Appl. Phys. Lett., 39, 73 (1981).
14. C. G. Newman, H. E. O'Neal, M. A. Ring, F. Leska and N. Shipley, Int. J. Chem. Kinetics, 11, 1167 (1979).
15. A. M. Beers and J. Bloem, Appl. Phys. Lett., 41, 153 (1982).
16. D. Adler, J. de Physique, 42, C4, 3-14 (1981).
17. S. Hasegawa, T. Kasajima and T. Shimizu, Phil. Mag., 3, 43, 149-56 (1981).
18. P. Hey and B. O. Seraphin, Solar Energy Materials, 3, 215-30 (1982).
19. H. Fritzsche, Sol. En. Mat., 3, 447-501 (1980).
20. B. A. Scott, J. A. Reimer, R. M. Plecenik, E. E. Simonyi and W. Reuter, Appl. Phys. Lett., 40, 973 (1982).
21. F. J. Kampas and R. W. Griffith, Appl. Phys. Lett., 39, 407 (1981).
22. P. C. Booth, D. D. Allred and B. O. Seraphin, J. Non-Cryst. Solids, 35-36, 213 (1980).
23. J. Tauc, in Optical Properties of Solids, ed. by F. Abeles, (North Holland, Amsterdam, 1970), p. 227-313.
24. M. Janai and B. Karlsson, Sol. En. Mat., 1, 387-95 (1979).
25. D. Adler, Hydrogenated Amorphous Silicon, ed. J. I. Pankove (in press).
26. D. L. Staepfer and C. R. Wronski, Appl. Phys. Lett., 31, 292 (1977).